encit 2020

ABCM Associação Brasileira de Engenharia e Ciências Mecânicas

18th Brazilian Congress of Thermal Sciences and Engineering
November 16-20, 2020 (Online)

# ENC-2020-0268
# FLAME IMAGE ANALYSIS FOR BIOMASS PELLETS COMBUSTION: ASSESSMENT BASED ON MORPHOLOGY VISUALIZATION

**Guilherme Henrique Dias Marques** [2]
**Robson Leal da Silva** [1,3]
[1] PEM / UEM – Graduate program in Mechanical Engineering (Research area: Thermal Sciences)
[2] UEM – Universidade Estadual de Maringá, Av. Colombo, 5790 – Zip Code: 87.020-900 – Maringá-PR, Brasil
[3] UFGD – Universidade Federal da Grande Dourados, Road MS-270, km 12 – Zip Code: 79.804-970 – Dourados-MS, Brasil
guilhermehenrique.d.m@gmail.com [2]; rlealsilva@hotmail.com [1,3]

***Abstract.*** *In this paper, we aim to evaluate flame morphology in a small burner of bio-fuel pellets collecting visual data from a cellphone camera, a set of thermocouples, and a load cell. Video from the experiment was processed on a frame-by-frame basis, different color modes were tested as means of pre-processing and a thresholding technique was applied to isolate the flame from the background. On our work, HSV color mode stood out as the most useful color mode in pre-processing. The low frame rate of the camera was able to capture some behavior on the flame's morphology, although not smoothly. Plotting of the visual data showed a valley in flame height and frontal area closely followed by a quick increase in the flame's brightness and size, possibly related to volatile and char combustion stages. The peak in temperature was delayed in regards to peaks in height and the flame's frontal area. Plotting of the accumulated frontal area exalted the points of quick increase in brightness and fuel burnout.*

***Keywords:*** *combustion, solid fuel, bio-fuel, image processing, diagnostic techniques*

## 1. INTRODUCTION

Nowadays, the desire for renewable energy sources has increased demand for biofuels, as fossil fuel reserves run out and environmental issues grow ever more concerning. Solid biofuels can be taken from plenty of agricultural processes, as husks, bagasse, and others, to be torrefied into dry, useful fuel of renewable source.

Combustion is required to convert solid fuels into thermal energy. Most biofuels derived from biomass present HHV ~20 $MJ.kg^{-1}$. There are also technological options, such as liquefaction and gasification to obtain liquid or gaseous fuel, typically with HHV reaching 30-60 $MJ.kg^{-1}$ and allowing better combustion performance. Intrusive and non-intrusive techniques are widely applied for assessments on combustion diagnosis, looking for temperature, air and flame speed, pressure, chemical species, and reaction kinetics, among others.

Computer-assisted image analysis is one of the non-intrusive techniques that can be used as a great tool to provide data about combustion experiments. Castiñeira et. al. (2012) have demonstrated a multivariable image analysis technique that assisted in identifying flame pixels on pictures of an industrial flare, and also trained a model capable of predicting combustion efficiency based on the image, crosswind velocity, and air injection rate. Chan et al. (2017) used a high-speed camera to visualize the combustion of single biomass particles and applied image analysis algorithms throughout several frames to note the variations in luminosity that are comparable to combustion stages of the biomass.

The step of correctly identifying the flame pixels is very important for image analysis. Gaidhane and Hote (2018) proposed an algorithm capable of identifying flame edges based on the red component of RGB images. Huang and Zhang (2010) used a thresholding technique on the HSV (Hue, Saturation, Value) color mode to separate different-colored parts of an ethylene flame from the picture background and with that, extracted information on the RGB (Red, Green, Blue) color mode, to evaluate flickering frequencies and correlating the RGB information with the fuel-air equivalence ratio. Also, Maynard and Butta (2017) proposed a physical model for flame height intermittency in buoyant diffusion flames, making use of an automated method to identify and measure the flame height from digital images.

The morphological characteristics of the flame are usually noted, even when automated image recognition does not take place. Recently, Sankaralingam et al. (2020) analyzed the combustion of benzoic resin solid fuel pellets, using a CCTV camera to record the experiment and proposed a mathematical model for evaluation and prediction of ignition, heat release rate and the flame structure, although flame length measurements were taken manually from the pictures, and not with automated software support. Dunn-Rankin and Chien (2019) analyzed the combustion characteristics of methane flames, noting morphological and color characteristics of the flame with a DSLR camera, but also taking measurements without image recognition software support. We believe image analysis can bring a significant improvement without much change to the experimental setup.

In this work we aim to identify and evaluate flame morphology in a small-scale experiment for biomass combustion, with different image pre-processing methodologies, taking parameters such as flame height and frontal area, that may provide an assessment of combustion performance as well as possible correlation to flame temperature and solid fuel consumption. We also aim to demonstrate how image analysis can be inexpensively added to combustion-related experiments where visual characteristics can be of interest, without much change to the experimental setup.

## 2. METHODS

### 2.1. Experiment Description

The assessment on this paper is part of a larger work, data and experimental support were provided by Júnior et. al. (2019). Samples of commercial pellets of residual peanut husk were burned in a small cylindrical burner (121mm length, 100 mm diameter). The burner has an opening for the insertion of a grill with a total airflow area of 1446.52mm$^2$ (~19% of total surface area, 91 holes of 4.5 mm in diameter). Another opening (19.5mm height, 67.5 mm width, 1316.25mm$^2$ total area) allowed for forced airflow provided by a fan in different flow rates and directed to the burner by a 3d-printed nozzle. 4 different flow rates were tested, as seen on Tab 1. Fan speed was measured by a tachometer. The videos were labeled v20, v25, v40, v50. A picture of the assembly, a model of the apparatus, and a picture of the grill are given in Fig 1 (a), (b) and (c) respectively. Measurements of average airspeed for video v20 were problematic, and a rough estimate is given at Tab. 1, as the discussion of the effects of the airspeed isn't on the scope of the current paper.

Table 1. Conditions of the experiment.

| Label | Flow rate [m$^3$/s] | Fan speed [rpm] | Average air speed [m/s] |
|---|---|---|---|
| v20 | 0.000134 | 144 | 0.1 (1) |
| v25 | 0.000402 | 286 | 0.3 |
| v40 | 0.001206 | 607 | 0.9 |
| v50 | 0.001742 | 874 | 1.3 |

(1) this value is roughly estimated, due to problems on the measuring process

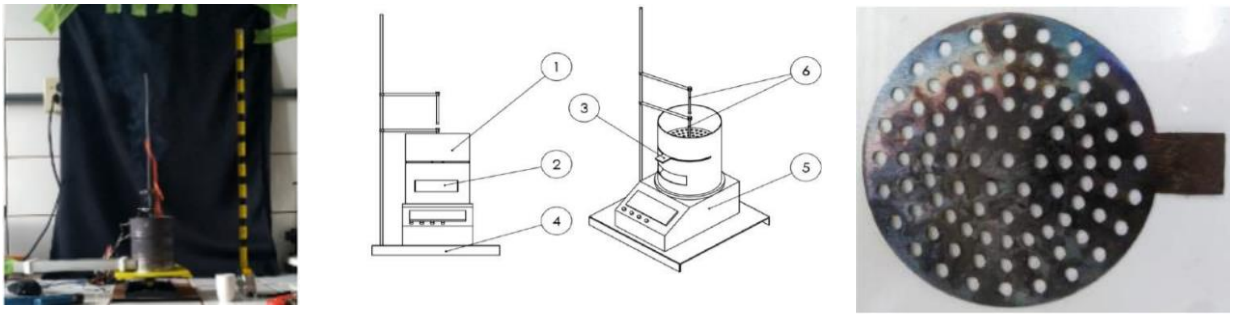


(a) (b) (c)

Figure 1. Pictures and illustration of the testing apparatus (a) picture of experiment with nozzle (joining the burner from the left) (b) assembly schematics (courtesy of Júnior, et. al. 2019) (b1) burner (b2) nozzle opening (b3) grill (b4) universal bracket (b5) load cell (b6) thermocouples (c) grill picture (courtesy of Júnior, et. al. 2019)

Data acquisition was made by two K-type thermocouples (-200 °C to 1260 °C measuring, ±2.2°C or 0.75% uncertainty) positioned at the grill (low thermocouple) and 60 mm above the burner (high thermocouple) and a load cell to measure mass during the combustion (0 to 5 kg range, 1g resolution). All components passed through a data acquisition system powered by a microcontroller board (ARMEGA2560) taking measures at 5 seconds intervals. To ensure ignition, a small amount of liquid fuel (~3.48g of alcohol 92.8% vol) was burned just below the airflow opening at the start of the experiment.

### 2.2. Image Processing

The experiment was recorded using a cellphone camera at 30 frames per second (fps) a black cloth was used as a contrasting background, and a ruler, marked every 50 mm was positioned beside the burner to allow measurements to be taken from the video, both are visible at fig 1 (a).

The video camera and the group comprising of the load cell and the thermocouples made for two separate data acquisition systems. The systems were synchronized by applying a disturbance on the load cell that was visible on both,

the video and the cell readings. Some error is expected as data from the load cell was taken every 5 seconds, and the video was recorded at 30 frames per second.

The video was analyzed frame-by-frame, in a MATLAB, the process is exemplified in fig. 2. The frames were segmented by thresholding, where a set of parameters were defined to identify each pixel as part of the flame ("on" pixel), or part of the background ("off" pixel). A different set of parameters could be used for different sections of the videos according to the brightness of the flame and lighting conditions of the room.

Typical segmentation steps would be, as shown in fig. 2, (i) framing the image (ii) converting to the desired color space (iii) erasing of undesirable objects (iv) thresholding using set parameters range (v) removal of noise by identifying small contiguous objects.

(a) (b) (c) (d) (e)

Figure 2. Main steps of segmentation (a) raw image (b) framed image (c) unwanted objects erased (d) segmented image (e) noise corrected image. The yellow line is the tallest point of the flame identified.

On the segmentation process, each frame was analyzed in RGB (red, green, blue) color mode, as imported into MATLAB, or pre-processed by converting to either HSV (Hue, Saturation, Value), YCbCr (Luma, Chroma Blue, Chroma Red) or L*a*b (SCIELAB color Space) color mode.

Whenever needed, objects difficult to separate from the flame (usually metallic, reflective, or colorful surfaces) caught within the video frame were erased from the video frames as part of the pre-processing (Fig. 2 (c)).

The parameters for thresholding would vary by lighting and flame conditions, and were manually set by testing an example frame extracted from the video. The parameters were a range of information on a pixel that would identify it as flame or background, for instance, on video v20, with HSV pre-processing and application of the erasing step, segmentation would be achieved by "turning on" pixels with the Hue color wheel parameter between 352.8° and 81.36°, Saturation parameter between 0 and 1, and Value parameter between 0.388 and 1.

The four videos of experiments were analyzed and labeled v20, v25, v40, and v50. The experimental runs differ in the flow rate of the forced airflow from under the burner. Height and frontal area data were obtained from the video. The height was obtained from the position of the tallest pixel considered to be part of the flame, and the frontal area was obtained by counting the segmented flame pixels, both measurements were assisted by the ruler visible in fig. 1 (a) and fig. 2 (a). That information is to be compared to temperature data at the K-type thermocouples, and mass from the load cell. Because of the shape of the burner, the flame is only visible starting 45 mm above the grill of the burner, therefore, a small portion of the frontal area and height of the flame was not visible on the video.

## 3. RESULTS AND DISCUSSION

Playing the videos, it was noted, at first, a faint reddish flame at the burner, that, at some point, would quickly change to a brighter, yellow and white tone. This point of fast change in brightness will be referred to as "Brightness Increase Frame" (BIF), and it's important for this paper because, due to the distinct visual properties before and after the BIF, a different set of thresholding parameters was needed before and after that point. Figure 3 shows a preview of each analyzed video and a visualization of the BIF.


(a.1)

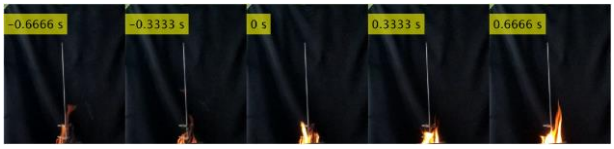


(a.2)

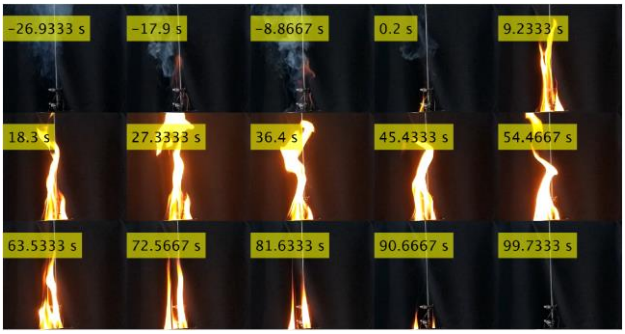


(b.1)

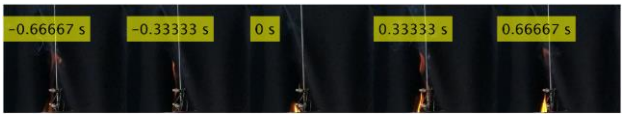


(b.2)

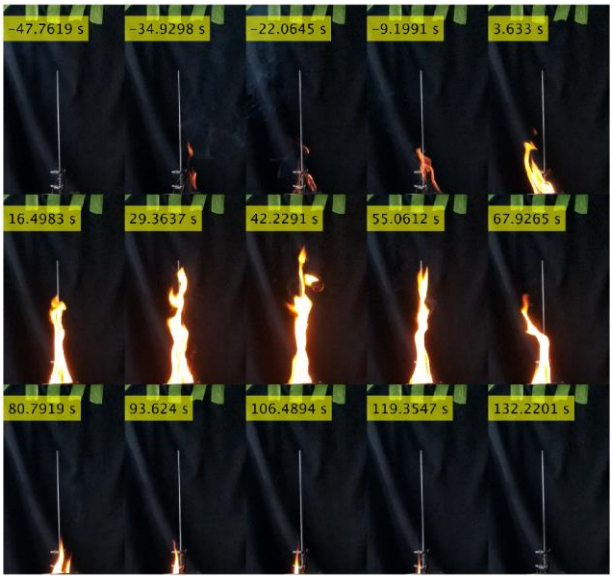


(c.1)


(c.2)


(d.1)

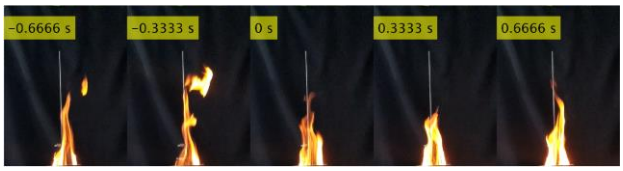


(d.2)

Figure 3. previews of videos (a.1) v20, (b.1) v25, (c.1) v40, (d.1) v50, and emphasis on the BIF (a.2) v20, (b.2) v25, (c.2) v40, (d.2) v50. Time zero is set at the BIF, and the first frame shown on the preview is the first frame with visible (above burner top) flame

The parameters for thresholding were tested in different pre-processing color modes (RGB, HSV, YCbCr, L*a*b). Figure 4 shows different results on the segmentation with different color modes in pre-processing of an example frame, taken from video v50, with and without the erasing process of the support bracket. Fig. 4 (b), (d), (f) shows how the reflecting bracket was harmful to the thresholding process as different color modes were unable to separate it from the actual flame, except for L*a*b, that was able to proper threshold the frame shown, and HSV, that minimized the impact of the bracket. The L*a*b color mode, however, would often need very precise parameters for good thresholding, resulting in parameters that would only be acceptable for a few frames at a time, and thus, not recommended to large portions of the video, as seen in Fig. 5, where another frame is tested using the same parameters as in Fig 4, in this case, L*a*b color mode mistakenly identifies the background, while the HSV continue to properly threshold. By erasing the support bracket, all color modes tested had a set of parameters that was able to reasonably identify the flame throughout the faint or the bright sections of the video, as seen in Fig 4 (c), (e), (g) and (i), pointing at the importance of being cautious with the visible background. The process of erasing the support bracket is at first, undesirable, as it also erased a small part of the visible flame, but in our experiment, this loss of flame was considered very minor and erasing the bracket was usually necessary to allow proper thresholding. Reflective objects are to be avoided in the future.


(a)

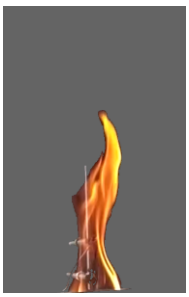
(b)


(c)

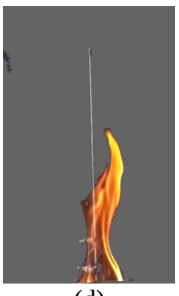
(d)


(e)


(f)


(g)

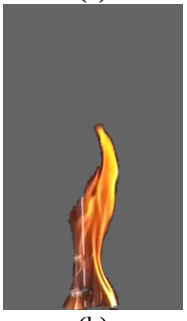
(h)


(i)

Figure 4 (a) original frame (b) using HSV (c) using HSV and erasing support (d) using YCbCr (e) using YCbCr and erasing support (f) using RGB (g) using RGB and erasing support (h) using L*a*b (i) using L*a*b and erasing support

(a) (b) (c)

Fig 5 (a) original frame (b) using L*a*b, same parameters as in fig. 4.h, the background is being mistaken as part of the flame (c) using HSV, same parameters as in Fig. 2.5, a small part of the support is still mistaken as the flame.

Although all color modes were able to identify the flame after the erasing process, the HSV stood out from the others, as its Hue domain allowed for easy selection of colors, as well as brightness control though the other parameters, moreover, the thresholding variables didn't need to be too finely defined to properly identify the flame, resulting in parameters that were largely applicable during the videos, and was often capable of thresholding without the erasing step, which was almost always needed in other color modes, due to reflections on the support bracket.

Figure 6 now concerns the post-processing of the data acquired, showing flame height data from video v20. Since 30 measures are taken every second, the resulting plot is quite noisy, as the flame often flickers faster than the time between frames, leading to very large and somewhat random variations from one frame to another. To better expose the behavior of the flame height, the figure also shows the averaged data on intervals of 1, 2.5, 5, and 10 seconds. the larger the averaging interval gets, the more information is lost, and as the averaging interval gets smaller, the plotting gets noisier, making it difficult to read. An averaging interval of 2.5 seconds seems to be a good compromise as of fig. 6. 2.5 seconds is also half the measuring interval of the thermocouples and load cell assembly.

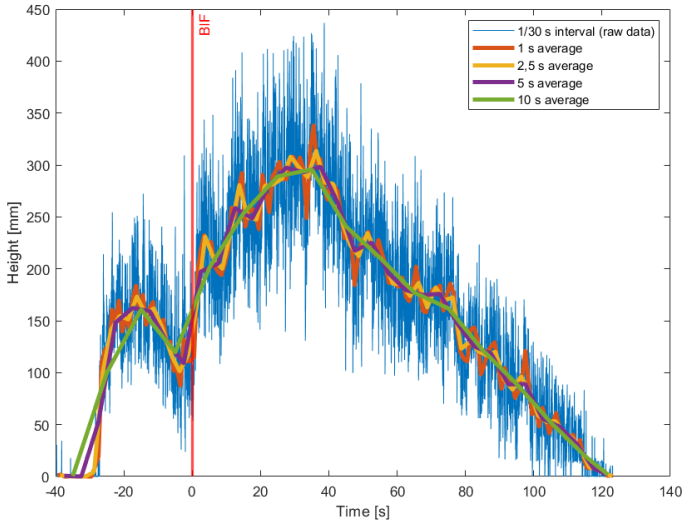


Figure 6. Flame height raw data, and averaged values plotted over. BIF is set as time zero.

Fig. 7 shows the flame height averaged in 2.5 intervals and the higher-positioned thermocouple temperature measure. A recurring behavior in 3 of 4 videos (v20, v25, and v40), is visible in Fig 7, which is the presence of 2 peaks in flame height, a local one before the BIF, and a global one after it. It's important to remember that flame height is only visible from 45 mm above the grill due to the shape of the burner. It's noticeable that the thermocouple curve experiences a change in slope soon after the BIF on most videos, but peaks several seconds after the peak in flame height. Also, the peak before the BIF is not present in the thermocouple temperature readings. Videos v25 and v40 showed very similar

behavior to video v20. On video v50, the peak of height before the BIF is not present and the "lag" between the height and temperature curves is significantly smaller than on videos v20 and v40

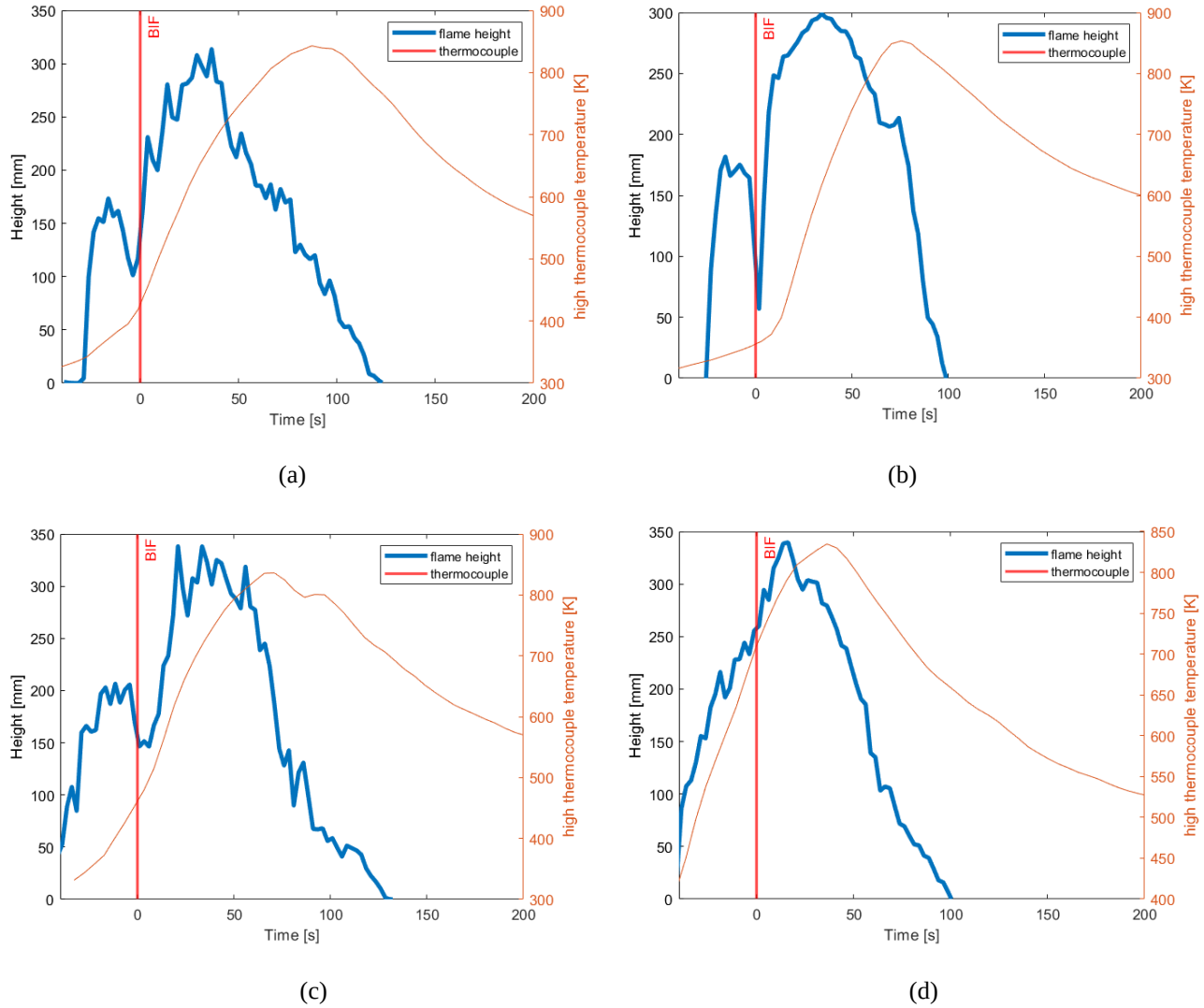


Figure 7. (v20) flame height and thermocouple temperature by time, height averaged on 2.5 seconds intervals (a) video v20 (b) video v25 (c) video v40 (d) video v50

The behaviors of the frontal area measurements were very similar to the height data, as seen in figure 8, although the frontal area curve had sharper inclinations, as are to be expected when comparing area measurements to length. Again, the peak before the BIF is present, as well as the lagged aspect of the thermocouple temperature. on video v50, a small local peak before the BIF can be seen in the frontal area plot, despite being absent in the height plot. We believe the twin peaks, now noted in all videos, to be the result of different stages of combustion. Shan et. al. (2018) measured the mean luminosity on the combustion of single particles of biomass (eucalyptus, pine, and olive resin) in a visual drop-tube furnace, and noticed very clearly two stages of combustion in all three biomasses, firstly a faint flame erupted, which the authors of that paper attribute to the combustion of volatile material, then, the flame extinguished and was very quickly followed by a new, much brighter flame, attributed to the char residue combustion stage of the particle. In that study, the combustion happened in a matter of milliseconds, as single particles were being observed. We believe the same behavior is happening here with the peanut husk combustion, the first peak in flame height and area would correspond to the volatile material combustion (before the BIF), and the second, much brighter and longer peak of height and area, would correspond to the combustion of char residue (after the BIF). Still on the paper by Shan et. al. (2018), two peaks in flame luminosity and size were noted on the devolatilization/volatile combustion stage of pine and eucalyptus particles, which according to them appear to correspond to the devolatilization of hemicellulose and cellulose. Our experiment could only identify a single peak in flame height and area before the BIF. Since there are significant quantities of hemicellulose and cellulose (Raju et. al., 2012) in the peanut husk, it is possible that a second peak would be hidden below the visible portion of the flame, or that both peaks happened too close to each other to be distinguished. Unfortunately, due to the non-

uniform lighting conditions in our experimentation room, the analysis of luminosity failed to provide meaningful data, as random variations were too common. A properly dark room or setup should be able to quantify the differences in brightness on the flames.

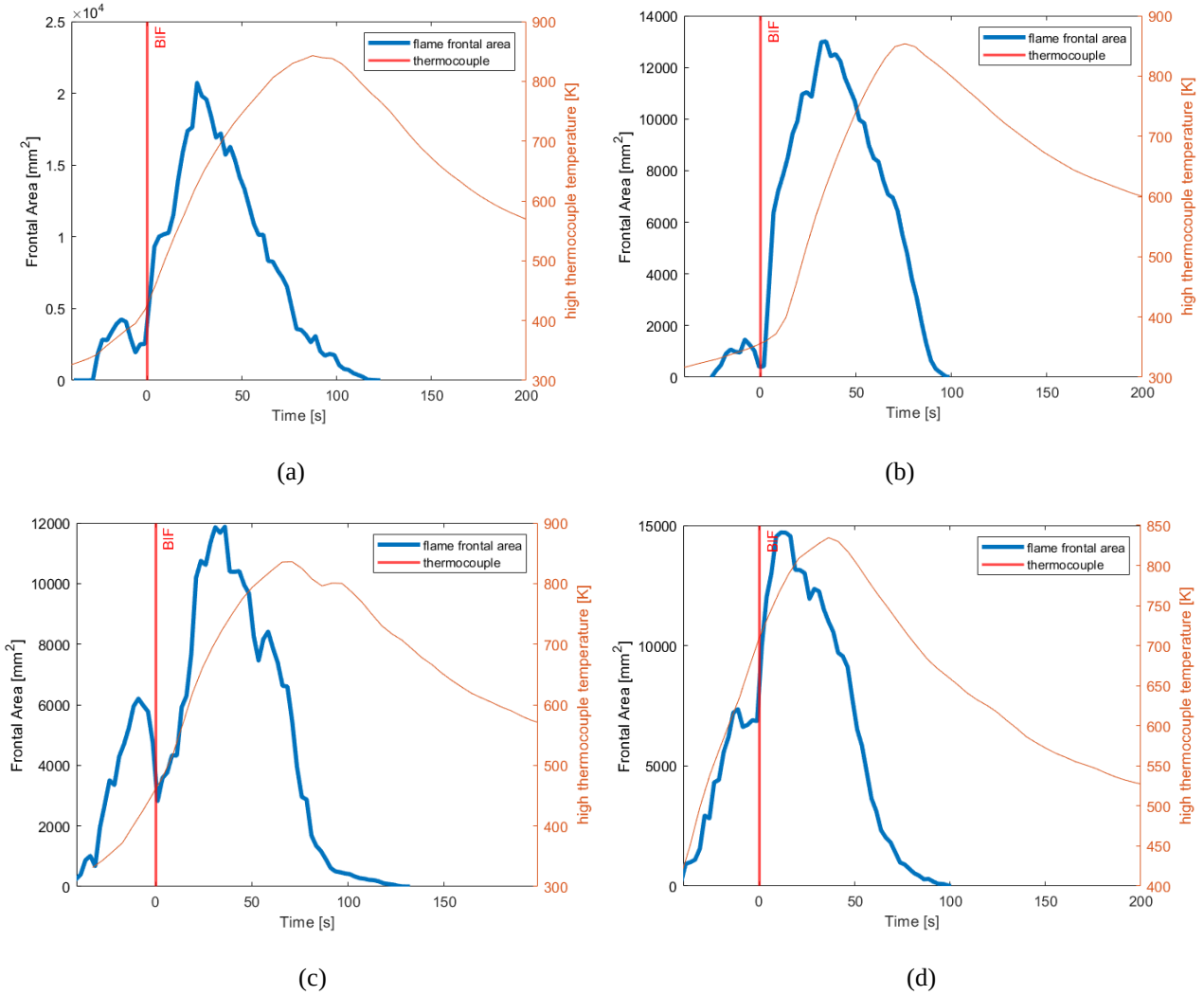


Figure 8. frontal area of flame and temperature by time. (a) video v20 (b) video v25 (c) video v40 (d) video v50, frontal area was averaged on 2.5 second intervals.

Since the flame is created from reacting fuel mass, it was thought to investigate information from accumulating the frontal area values (where the accumulated flame frontal area at a given point in time is given by the sum of all previously measured flame frontal areas). We see in figure 9, the behavior of the accumulated frontal area curve in comparison to the mass measured by the load cell. There we notice two very distinct inclinations on the mass curve. As volatile material burns out, mostly slow-burning carbon remains in the fuel, resulting in the flattened aspect by the end of the video. That flattening happens roughly at the same time in the measured mass curve and the accumulated mass curve. It's also noticeable a rapid increase on the slope of the accumulated mass curve around the time of the BIF, (not present in the measured mass curve), this could be influenced by the change in thresholding parameters at the time of the BIF, however, a factual increase in the flame's frontal area is visible in fig. 3, so the influence of the change in parameters should be very small. That change in slope is followed by a mostly uniform climb until the material is mostly extinguished, and the accumulated frontal area curve also mostly flattens, until the flame falls below the visible line of the burner.

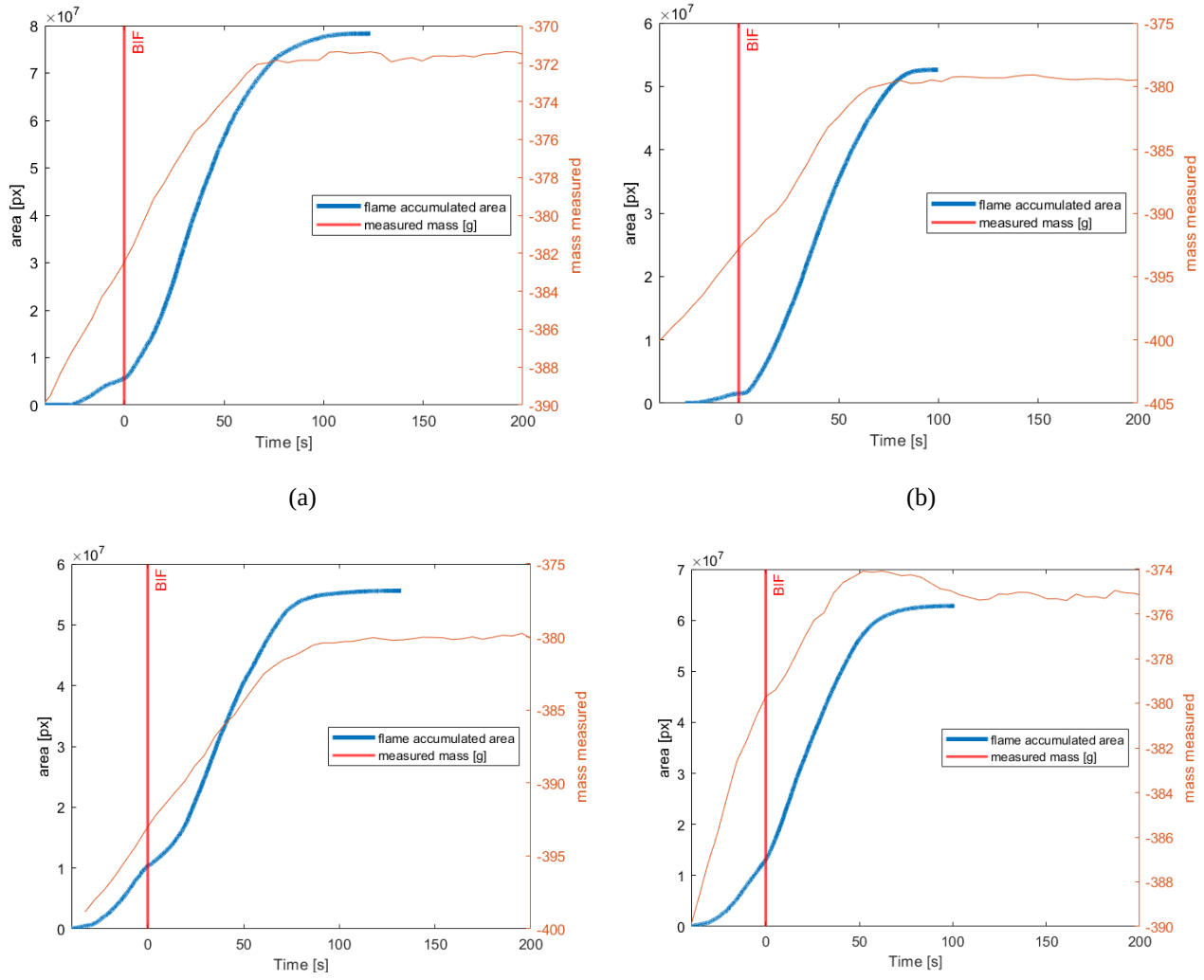


Figure 9. accumulated frontal area and measured mass on videos (a) video v20 (b) video v25 (c) video v40 (d) video v50

## 4. CONCLUSIONS

Of the color modes tested during pre-processing, HSV stood out as the most effective, as it allowed for easy selection of colors and brightness during thresholding, as well as mitigating the problem of unwanted objects on the frame. An opaque black coating should probably be applied to unwanted objects on future experiments to simplify the thresholding. The recording at 30 frames per second was too little to allow for smooth visualization of the flame's movement, and taking average values for height and frontal area every 2.5 seconds was a good compromise between fidelity to the raw data and visualization of the flame's behavior. The height data showed a significant delay between the peak in height and maximum temperature on the thermocouple, which occurred later. Two peaks in the flame`s frontal area were noted on all 4 videos, and analogous peaks in height were noted in 3 of the 4 videos, those are believed to be related to the volatile and char residue combustion stages. The accumulated frontal area showed steep changes in inclination upon reaching the brightness increase frame (BIF) and burnout of the biomass and could be an indirect indicator of burnout.

## 5. ACKNOWLEDGEMENTS

To scholarship for undergraduate engineering students (IC & ITI) from UFGD and CNPq - National Council for Scientific and Technological Development, and support to PEM / UEM from CAPES (Coordination for the Improvement in Higher Education Personnel).

## 6. REFERENCES

Castiñera, D., Rawlings, B. C. and Edgar T. F., 2012. "Multivariarive Image Analysis (MIA) for industrial Flare Combustion Control". *Industrial & Engineering Chemistry* Research Vol. 51 Issue 39, 12642-12652 DOI: 10.1021/ie3003039

Chien Y. C., Rankin, D. D. 2019, "Combustion Characteristics of Methane Hydrate Flames" *Energies – Open Access Journal*, Vol 12, Iss 10, 1939. DOI: 10.3390/en12101939

Gaidhane, V. H. and Hote, Y. V., 2018. "An efficient edge extraction approach for flame image analysis*" patter analysis and Applications*, Vol. 21, 1139-1150. DOI: 10.1007/s10044-018-0717-0

Huang, H.W. and Zhang, Y., 2010. "Dynamic application of digital image and colour processing in characterizing flame radiation features". *Measurement Science and Technology*, Vol. 21, 085202. DOI: 10.1088/0957-0233/21/8/085202

Júnior, D. M., Ribeiro, N. M., Coradini, M. F., Silva, R. L., Olieira, J. C. D. and Conceição, W. A. S. 2019, "Pellets Combustion in a Small Size Burner: Performance Evaluation". *25th ABCM International Congress of Mechanical engineering – COBEM 2019*. Uberlândia, Brazil

Maynard, T. B. and Butta, J. W., 2018. "A physical Model for Flame Height Intermittency" *Fire Technology*, Vol 54, p.135-161 DOI: 10.1007/s10694-017-0678-7

Raju G. U., Kumarappa S., Gaitonde V. N., "Mechanical and physical characterization of agricultural waste reinforced polymer composites", *J. Mater. Environ*. Sci., 3, 2012, 907-916. ISSN: 2028-2508.

Sankaralingam, R., Sengottuvelan B., Venkat, P., Selvaraj, M., Arunachalam V., Natarajan, J. 2020, "Experimental investigation on varying flame characteristics of benzoic resin solid fuel pellets", *Renewable Energy*, Vol 147, p. 1500-1510. DOI: 10.1016/j.renene.2019.09.061

Shan, L., Kong, M., Bennet, T. D., Sarroza, A. C., Eastwick, C., Sun, D., Lu, G., Yan, Y. and Liu, H., 2018. "Studies on combustion behaviours of single biomass particles using a visualization method" *Biomass and Bioenergy*, Vol. 109, p.54-60. DOI: 10.1016/j.biombioe.2017.12.008

## 7. RESPONSIBILITY NOTICE

The authors are the only responsible for the printed material included in this paper.